^{99m}Tc-Labeled Bevacizumab *via* HYNIC for Imaging of Melanoma

Ximena Camacho[a], María Fernanda García[a,b], Victoria Calzada[a], Marcelo Fernández[a], Omar Alonso[c], Juan Pablo Gambini[c], Rodrigo Barbosa de Aguiar[d], Camila Maria Longo Machado[e], Roger Chammas[d], Williams Porcal[b] and Pablo Cabral[a,*]

[a]*Departamento de Radiofarmacia, Centro de Investigaciones Nucleares, Facultad de Ciencias, Universidad de la República, Mataojo 2055, 11400 Montevideo, Uruguay*

[b]*Laboratorio de Química Orgánica, Facultad de Ciencias-Facultad de Química, Universidad de la República, Mataojo 2055, 11400 Montevideo, Uruguay*

[c]*Centro de Medicina Nuclear, Hospital de Clínicas "Dr. Manuel Quintela", Facultad de Medicina, Universidad de la República, Av. Italia s/n, 11600, Montevideo, Uruguay*

[d]*Laboratório de Oncologia Experimental, Faculdade de Medicina, Universidade de São Paulo, Av. Dr. Arnaldo Nº 455- Cerqueira César - CEP: 01246903, São Paulo, Brazil*

[e]*Nuclear Medicine Medical Investigation Laboratory LIM43-Hospital das Clínicas da Faculdade de Medicina da Universidade de Sao Paulo - HCFMUSP, Brazil*

Abstract: Vascular endothelial growth factor (VEGF) is one of the classic factors to tumour-induced angiogenesis in several types, including melanoma. Bevacizumab, a monoclonal antibody anti-VEGF, could be used as an imaging tool in clinical studies. The aim of this study was to radiolabeled Bevacizumab with ^{99m}Tc and evaluate it *in vivo* imaging properties. Bevacizumab was derivatized with the activated ester succinimidyl-hydrazinonicotinamide hydrochloride (Suc-HYNIC) as a bifunctional coupling agent. A mixture of Tricine/$SnCl_2.2H_2O$ was added to Bevacizumab-HYNIC and radiolabeled with $^{99m}TcO_4^-$. The radiochemical stability of the radiolabeled sntibody was assessed. Biodistribution studies and SPECT-CT imaging were evaluated in healthy and tumor-bearing C57BL/6J mice at 1, 4 and 24 h (n =5). We demonstrated that ^{99m}Tc-HYNIC-Bevacizumab was stable over 24 h in solution and serum. *In vivo* biodistribution studies revealed tumor-to-muscle ratios of ^{99m}Tc-HYNIC-Bevacizumab was 9.28, 17.19 and 8.51 at 1, 4 and 24 h p.i. SPECT/CT imaging of tumor-bearing C57BL/6J mice showed tumor selective uptake of ^{99m}Tc-HYNIC-Bevacizumab. ^{99m}Tc-HYNIC-Bevacizumab could become a potential radiopharmaceutical to evaluate the expression of vascular endothelial growth factor (VEGF) in solid tumors and could be seen as a clinic tool for the screening of solid tumors that might respond to the Bevacizumab chemotherapy.

Keywords: Melanoma, Angiogenesis, Bevacizumab, HYNIC, organic synthesis, technetium-99m.

1. INTRODUCTION

Angiogenesis is a complex process by which in physiological conditions, new blood vessels are form from a pre-existing vasculature [1-4], being one of the mechanisms by which the organisms assures the supply of nutrients and oxygen [5,6].

However it is also implicated in the pathogenesis of a variety of disorders including cancer, wound healing, and inflammation. Tumour angiogenesis is a continuous process which allows tumor cells to execute their critical growth by supplying the tumour with nutrients and oxygen and providing a route for metastatic spreading [2,3].

Vascular endothelial growth factor (VEGF) has been extensively studied as one of the most important proteins involved in the development of the physiological and pathological angiogenesis [7-15]. The VEGF family includes VEGF-A, -B, -C, -D, and placental growth factor. VEGF-A (hereafter referred as VEGF) has been the most studied and is one of the key growth factors involved the development and maintenance of tumour angiogenesis [8,10,11,16-18].

Overexpression of VEGF occurs in many human tumours types, suggesting that this diffusible molecule is a rational target for antiangiogenic therapy [19-21]. This has led to the development of antiangiogenic strategies that allow neutralization of this factor, which is the case of the monoclonal antibody Bevacizumab (rhuMAb-VEGF, Avastin®, Genentech, USA) [22]. Bevacizumab is a recombinant humanized monoclonal antibody that binds to all VEGF isoforms with high affinity and thereby blocks ligand-receptor signalling [21]. Bevacizumab was the first Food and Drug Administration-approved clinical agent to target tumour angiogenesis and has been registered in February 2004 for the first-line treatment of metastatic colon-

*Address correspondence to this author at the Laboratorio de Radiofarmacia, Centro de Investigaciones Nucleares, Facultad de Ciencias, Universidad de la República, Montevideo, Mataojo 2055, P.O. 11400, Montevideo, Uruguay; Tel: (+5982) 5250901/108; Fax: (+5982) 5250895; E-mail: pcabral@cin.edu.uy

rectal cancer in combination with Fluorouracil (5-FU)-based chemotherapy [22,23].

Melanoma causes more than 75% of all skin cancer deaths [24-26]. There are approximately 133,000 new cases of melanoma worldwide each year [27,28]. It is clear the necessity of studies for the development of new treatment options more effective in fighting this disease. Several studies point to a role for VEGF in melanoma. Its expansion is associated with advanced disease, tumour burden, poor overall survival and probability of progression. Tumor progression in melanoma is a multistep process involving proliferation, neovascularisation, lymphangiogenesis, invasion, circulation, embolism, and extravasations [29]. The mechanisms responsible for the antitumor activity of conventional therapy and the biology of the tumour are not fully understood. In this way, the development of new anti-VEGF imaging strategies is of potential interest in the treatment of melanoma and could help advance our understanding of cancer and providing longitudinal monitoring of the tumour response.

One strategy that has been considered in oncology is the use of radiolabel proteins for the purpose of monitoring anticancer therapies as well as to better understands the tumour progression and invasion [9]. VEGF imaging could provide non-invasively insight in the local VEGF status and thereby be useful to guide antiangiogenic therapy. Recently, tumor visualization and *in vivo* measurement of VEGF tumour levels was possible by using radionuclide VEGF imaging [30-35].

Great availability, well-established labelling chemistries and easy access are important pre-conditions for the implementation of a radionuclide into diagnostics practices. Technetium-99m has suitable nuclear properties for molecular imaging, due to its favourable physical characteristics [t½ = 6.04 h, Eγ = 140 Kev (89 %)] [36] and to its inexpensive cost and readily availability in any medical centre.

The aim of this study was to describe the development and the *in vivo* evaluation of ^{99m}Tc-bevacizumab in a tumor-bearing mouse model of melanoma. For this purpose, we optimize the radiolabeling of Bevacizumab with ^{99m}Tc, using HYNIC as a bifunctional chelating agent. The HYNIC group is attractive for preparing ^{99m}Tc-labeled peptides and proteins with a high efficiency and *in vivo* stability for medical imaging [37,38]. HYNIC can coordinate to technetium through pyridyl nitrogen and hydrazine nitrogen and requires the use of a coligand (i.e. tricine, ethylenediamine diacetic or phosphines) to complete the coordination sphere around the metal. HYNIC can be coupled *via* the carboxylic function to free amine groups of lysine side chains and N-terminal residues, thus forming a bridge between the biomolecule and the technetium centre. Conventionally, HYNIC is coupled with amine groups using an activated ester, such as the Suc-HYNIC (Scheme **1**).

2. MATERIALS AND METHODS

2.1. Organic Synthesis of HYNIC Analogues

Proton NMR spectra were recorded on a Bruker DPX-400 spectrometer. The chemical shifts values are expressed in ppm relative to tetramethylsilane as internal standard. Mass spectra were determined on a

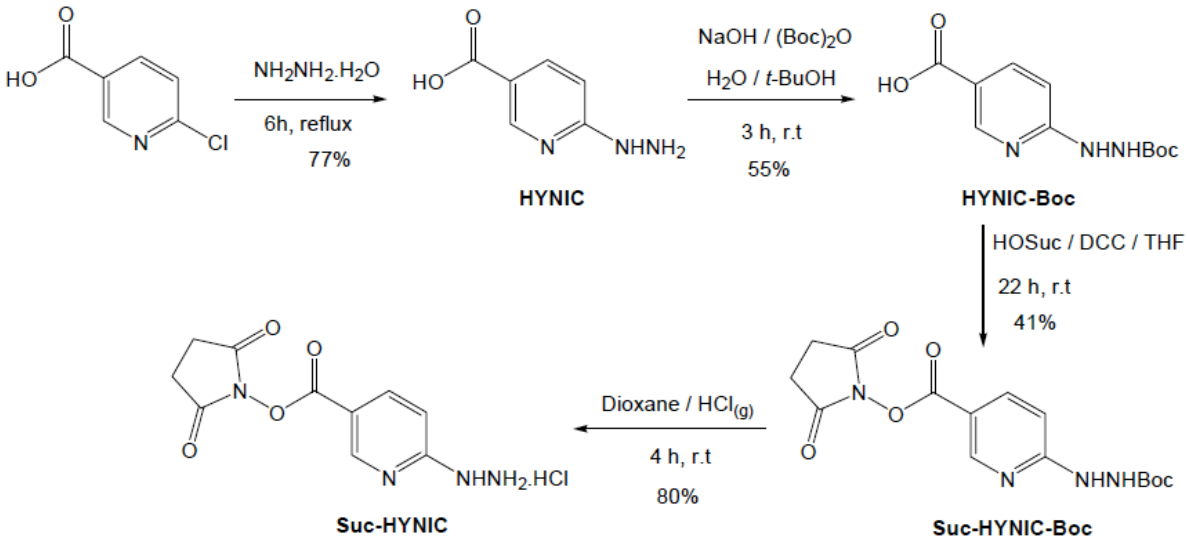

Scheme 1: Synthesis of activated ester Suc-HYNIC.

LC/MSD-Serie 100 Hewlett-Packard spectrometers using electrospray ionization (ESI).

6-Hydrazinopyridine-3-carboxylic Acid (HYNIC)

A suspension of 6-Chloronicotinic acid (1 g, 6.3 mmol) and 60-65 % hydrazine monohydrate (10.6 mL, 113.0 mmol) was heat a reflux for 6 h. After cooling to room temperature, the aqueous phase was acidified to pH 5.5 by slow addition of 12 N HCl and the resulting solid was isolated by filtration and washed with 95% ethanol and diethyl ether. After the workup, the residue corresponding to the 6-Hydrazinopyridine-3-carboxylic acid (pure by TLC and ^{1}H-NMR), was used in the next reaction without further purification. The solid was dried at reduced pressure to give a yellow pale solid (0.749 g, 77 %). ^{1}H NMR (DMSO-d6) δ (ppm): 6.70 (d, *J*= 8.4 Hz, 1H, H-5), 7.86 (dd, *J*= 8.8 Hz, *J* = 2.0 Hz, 1H, H-4), 8.32 bs, 1H, NH), 8.52 d, *J*= 1.6 Hz, 1H, H-2); ESI-MS, *m/z*: 154 ($M^{+\cdot}$ + H).

6-(1-tert-butoxycarbonyl)hydrazinopyridine-3-carboxylic Acid (HYNIC-Boc)

To a solution of **HYNIC** (0.150 g, 0.98 mmol) in a mixture of water (1 mL), *t*-BuOH (1 mL), and NaOH (0.045 g, 1.13 mmol) was added di-*tert*-butyl dicarbonate (0.224 g, 1.03 mmol) and the final mixture was stirred during 3 h at room temperature. The mixture was concentrated to half its original volume with vacuum evaporation, the aqueous phase was acidified to pH 5 by slow addition of cold 1 N HCl, and the resulting mixture was extracted with EtOAc. The combined organic layers were dried over Na_2SO_4, filtered, and concentrated. The residue was purified by column chromatography (SiO_2, mixture of petroleum ether:EtOAc), yielding **HYNIC-Boc** as a yellow pale solid (0.136 g, 55 %). ^{1}H NMR (Acetone-d6) δ (ppm): 1.45 (s, 9H), 6.76 (d, *J* = 8.4 Hz, 1H, H-5), 8.11 (d, *J* = 8.8 Hz, 1H, H-4), 8.15 (s, 1H, NH), 8.26 (s, 1H, NH), 8.73 (d, *J* = 0.8 Hz, 1H, H-2); ESI-MS, *m/z*: 254 ($M^{+\cdot}$ + H).

Succinimidyl 6-(1-tert-butoxycarbonyl)hydrazine-pyridine-3 Carboxylic Acid (Suc-HYNIC-Boc)

A mixture of **HYNIC-Boc** (0.240 g, 0.949 mmol), HOSuc (0.109 g, 0.949 mmol) and DCC (0.195 g, 0.949 mmol) in dry THF (8 mL) was stirred during 22 h at room temperature. The DCU precipitate was removed by filtration and the solvent removed *in vacuo*. The residue was purified by column chromatography (SiO_2, mixtures of petroleum ether/EtOAc) yielding **Suc-HYNIC-Boc** as a cream solid (0.137 g, 41%). ^{1}H NMR (Acetone-d6) δ (ppm): 1.46 (s, 9H), 2.95 (s, 4H), 6.85 (d, *J*= 8.8 Hz, 1H, H-5), 8.18 (dd, *J*= 8.8 Hz, *J*= 1.6 Hz 1H, H-4), 8.38 (s, 1H, NH), 8.55 (s, 1H, NH), 8.81 (d, *J*= 2.0 Hz, 1H, H-2); ESI-MS, *m/z*: 351 ($M^{+\cdot}$ + H).

Succinimidyl 6-hydrazinopyridine-3-carboxylic Acid Hydrochloride (Suc-HYNIC)

Firstly, a solution of HCl in dioxane was prepared by bubbling HCl into dry dioxane with molecular sieves (5A) for 20min. A mixture of **Suc-HYNIC-Boc** (0.1 g, 0.286 mmol) and HCl/dioxane (4 mL) was stirred during 4 h protected from ligth at room temperature. The cloudy reaction was carefully filtered and the solid product was extensively washed with EtOAc and dry diethyl ether. The white solid (65 mg, 80%) obtained was dried under high vacuum and stored at -20ºC. ^{1}H NMR (DMSO-d6) δ (ppm): 2.89 (s, 4H, CH_2), 7.00 (d, *J* = 8.8 Hz, 1H, H-5), 8.21 (d, *J* = 8.8 Hz, *J* = 2.4 Hz, 1H, H-4), 8.87 (d, *J* = 2.0 Hz, 1H, H-2), 9.50 (s, 1H, NH), 10.54 (s, 2H, NH). ESI-MS, *m/z*: 251 ($M^{+\cdot}$ + H).

2.2. Conjugation HYNIC-Bevacizumab

Bevacizumab (Avastin®) 25 mg/mL produced by Genetech, Inc., was provided by Roche Laboratories. Suc-HYNIC-Bevacizumab conjugation reaction was initiated by adding 33 µL of 1M $NaHCO_3$ to 0.067 µmol of Bevacizumab in 0.4 mL. To this 0.33 µmol Suc-HYNIC in 7.1 µL DMSO (J. T. Baker) were added. The mixture was incubated at 18 – 25 ºC for 30 minutes at darkness, pH 8. The conjugated was purified from free HYNIC in a Sephadex G-25 size exclusion chromatography (SEC) (PD-10, Amersham Biosciences). The purified was lyophilized and store 4ºC (solution A). 4800 MALDI TOF/TOF (Abi Sciex) lineal acquisition was used to determine the level of *HYNIC* conjugation to Bevacizumab.

2.3. Radiolabeling of HYNIC-Bevacizumab and Quality Controls

For optimal radiolabeling conditions, 44.6 µmols of Tricine (N-[Tris(hydroxymethyl)-methyl]glycine, Sigma) were dissolved in 0.8 mL water (pH adjusted to 4.5-5 with 0,05 mL HCl 2.0 M). In a second vial 44.3 µmols of $SnCl_2.2H_2O$ (J. T. Baker), were dissolved in 0.5 mL HCl 2.0 M and 0.05 mL of this solution was added to the Tricine vial. Finally the volume was adjusted to 10 mL with saline (solution B). 25 µL of Solution B was added to 6.7 nmol of conjugated antibody, and immediately $Na^{99m}TcO_4$ solution (TecnoNuclear ^{99}Mo-^{99m}Tc generator), in not more than 1 mL. The mixture pH 5-6 was incubated at room temperature for 30 minutes. Different levels of activity 70, 111, 203 and 525 MBq

per mg of antibody were assay to evaluate the maximal specific activity. The samples were measured in a Dose Calibrator Capintec CRC7, Solid Scintillation counter with 3"x 3" NaI(Tl) crystal detector associated to a ORTEC multichannel analyzer.

Radiochemical purity of the labeled biomolecule was assessed by chromatography using ITLC-SG and NaCl 0,9 % ([Rf=0, $^{99m}TcO_2.H_2O$ and ^{99m}Tc-HYNIC-Bevacizumab], [Rf=1, ^{99m}Tc-Tricine and $^{99m}TcO_4^-$]), ITLC-SG (Pall Corporation) saturated with bovine serum albumin (BSA, Sigma-Aldrich) and EtOH:NH_3:H_2O (2:1:5) ([Rf=0, $^{99m}TcO_2.H_2O$], [Rf=1 ^{99m}Tc-Tricine, $^{99m}TcO_4^-$ and ^{99m}Tc-HYNIC-Bevacizumab]), and Whatman Nº 1 paper (Whatman International Ltd) and MEK ([Rf=0, $^{99m}TcO_2.H_2O$, ^{99m}Tc-Tricine and ^{99m}Tc-HYNIC-Bevacizumab], [Rf=1, $^{99m}TcO_4^-$]) as stationary and mobile phase respectively.

Also the radiochemical purity and characterization of ^{99m}Tc-HYNIC-Bevacizumab were carried out on a side exclusion chromatography (SEC) as well as on HPLC. SEC was performed on a PD-10 column equilibrated and eluted with normal saline, at a flow rate of 1.0 mL/min. The eluate was collected in fractions of 1 mL and its radioactivity measured in an automatic gamma counter (Capintec CRC-7; Montvale, NJ, USA). The HPLC measurements were obtained with a Protein-Pak 300 SW 7.5 mm x 30 cm column (Waters) with isocratic mode phosphate buffer 0.05 M, pH 7.0, 0.7 mL/min flow rate, equipped with UV absorbance and NaI(Tl) scintillation detectors.

2.4. Stability of ^{99m}Tc-HYNIC-Bevacizumab

The integrity of this radiolabeled antibody was analyzed in normal saline and in serum. ^{99m}Tc-HYNIC-Bevacizumab was incubated with 0.9% NaCl at 37ºC and the reaction mixture was assayed by HPLC measurements as mentioned above for different time points from 1 to 24 h. The in-vitro stability in serum (Gibco, USA) was assayed in a similarly, with the percentage of [99mTc]-free or bound to Bevacizumab also measured by HPLC measurements.

2.5. L-Cysteine Challenge Assay

The radiochemical stability of ^{99m}Tc-HYNIC labeled Bevacizumab was tested in a challenge assay, performed essentially as described by Hnatowich *et al*. [39]. The L-Cysteine challenge evaluated by incubation in 90 µL (3.7 MBq) of ^{99m}Tc-HYNIC-Bevacizumab with 10 µL of L-Cysteine 1 and 10 mM (Sigma-Aldrich, USA), final concentration of L-Cysteine was 0.1 and 1 mM. The reactions were occurred at 37ºC for different time points from 1 to 24 h and evaluated by HPLC measurements as mentioned above.

2.6. Tumor-Bearing Mice Model

For biodistribution studies with ^{99m}Tc-HYNIC-Bevacizumab were conducted in subcutaneous murine melanoma model. Briefly, viable $1x10^6$ B16-F1 cells (murine melanoma cell line obtained from the American Type Culture Collection) were injected subcutaneously in the right leg of C57BL/6J, in a volume of 100 µL. For SPECT/CT image studies with ^{99m}Tc-HYNIC-Bevacizumab, viable $7,5 \times 10^5$ B16-F10 cells (murine melanoma cell line obtained from the American Type Culture Collection) were injected subcutaneously in the left lateral of thorax of C57BL/6J, in a volume of 100 µL.

C57BL/6J male mice, 8-10-weeks-old (20-24 g), were obtained from the Animal House Facility of the Universidad de la Republican-Uruguay and from Bioterio Central da Faculdade de Medicina-USP. Mice were maintained with food and water *ad libitum* throughout the experiments, in a temperature- and humidity-controlled room. All procedures involving animals were approved by the local Animal Experimentation Ethics and Animal Care and Use Committees. Tumours with an average longest dimension of 1 cm were used in the experiments.

2.7. *In Vivo* Biodistribution Studies

The biodistribution of ^{99m}Tc-HYNIC-Bevacizumab was determined in healthy and B16-F1 tumor-bearing C57BL/6J mice. Animals (n=5 per group) were injected in the tail vein with approximately 7.4 MBq of radiolabelled Bevacizumab and euthanized by cervical dislocation after 1, 4 and 24 h. Selected tissues (tumor, heart, liver, lungs, thyroid, kidneys, stomach, spleen, gastrointestinal tract and bladder) were excised, rinsed of residual blood, weighed and their radioactivity measured in a NaI(Tl) detector. Urine and blood were also collected and measure. Uptake of radioactivity in the tumor and normal tissues was expressed as percentage of the injected dose (% ID) and as percentage of the injected dose per gram of tissue (% ID/g).

2.8. SPECT/CT Mice Images with HRES and Multi-Pinhole Collimators Acquisitions and Analysis

SPECT/CT imaging studies were performed by injecting 37-55.5 MBq of ^{99m}Tc-HYNIC-Bevacizumab

into the tail vein of B16-F10 melanoma-bearing mice. After 6 and 24 h post-injection, the animals (n=3 per time) were anesthetized with a gas mixture (air and 1–1.5% isoflurane) and submitted to SPECT/CT images. All images data were acquired 24 h after ^{99m}Tc-HYNIC-Bevacizumab injection using HRES collimators with 1.4mm, 127x127 mm trans-axial field of view, 64 projections with >9Kctps each all animals with an Triumph microSPECT/CT (Gama Medica). Acquired images were analyzed by Amide with same threshold parameters (75%) for data interpretation.

Also images data were acquired 24h after radiotracer injection on Triumph microSPECT/CT using dual sodium idiode crystals in combination with a multi-pinhole with 1 mm each aperture and a radius of rotation of 5.5 cm, followed by CT acquisitions. Acquired images were reconstructed with filter OSEM correction following an Amira DICOM generation and analyzed Amide with same threshold parameters (75%) for data interpretation [40].

2.9. Statistical Analysis

Results were expressed as mean ± standard error, as indicated. Statistical analysis was done using the unpaired t test. A p-value ≤ 0.05 was considered significant.

3. RESULTS

3.1. Organic Synthesis of HYNIC Analogues

First, standard procedure for synthesis de **HYNIC** involve the nucleophilic displacement of the halogen of 6-chloropyridine 3-carboxylic acid by means of hydrazine in great excess under reflux for several hours (77%, Scheme **1**). Due to the zwitterionic character of **HYNIC** was assayed a typical Boc-protection of amino acids. **HYNIC-Boc** was synthesized using di-(*tert*-butyl) dicarbonate $(Boc)_2O$ under basic condition in presence of a mixture *t*-BuOH/H_2O as solvents (Scheme **1**). The activated ester **Suc-HYNIC-Boc** was obtained by reaction of the corresponding acid and *N*-hydroxysuccinimide (HOSu) in the presence of dicyclohexyl carbodiimide (DCC). Finally, **Suc-HYNIC** was obtained through deprotection of the Boc derivative under acidic conditions.

3.2. Conjugation of HYNIC-Bevacizumab

Suc-HYNIC was conjugated to Bevacizumab at room temperature for 30 min. A PD10 column was used to separate the HYNIC-Bevacizumab conjugate from free HYNIC. More than 80% of the initial amount of monoclonal antibody was recovered as monitored by UV absorbance at 280 nm using a molar extinction coefficient of 1.4. The m/z ratio of HYNIC-Bevacizumab for the $(MH)^+$ was 149605.7 and $(MH)^+$ for Bevacizumab is 149116.9 used as a reference, resulting in 4 molecules of HYNIC per antibody molecule (Figure **1A** and **1B**).

3.3. Radiolabeling and Stability of ^{99m}Tc-HYNIC-Bevacizumab

^{99m}Tc-HYNIC-Bevacizumab was purified and had its chemical identity accessed by size-exclusion chromatography (SEC) and HPLC. Radiochemical purity exceeded 90 % in all the experiments. SEC analysis shown ^{99m}Tc-radiolabeled Bevacizumab elutes from the column at a retention volume of 4-5 mL, whereas free $^{99m}TcO_4^-$ and ^{99m}Tc-Tricine resulting a peak at 8-9 mL (Camacho *et al.* 2012). In the HPLC system, radiochromatograms revealed R_t values of 13.19 min, 11.86 and 7.82 min for $^{99m}TcO_4^-$, ^{99m}Tc-Tricine and ^{99m}Tc-HYNIC-Bevacizumab, respectively (Figure **2**, **B.1** and **B.2**). The peak of radioactivity obtained at 7.82 min overlaps with the UV trace (280 nm; 7.74min) for ^{99m}Tc-HYNIC-Bevacizumab (Figure **2A**).

Different levels of activity were assayed to evaluate optimal radiolabeling conditions; yields higher to 80% were obtained with activities lower than 525 MBq/mg. The optimal condition observed showed a specific activity of 111 MBq/mg with a 90±1 % labeling yield [41]. *In vitro* radiochemical stability studies of ^{99m}Tc-HYNIC-Bevacizumab showed that the radiolabeled antibody complex was stable over a 24 h time period in NaCl 0.9% 37ºC, showing a variation in the integrity of the complex of only 2 % at 4 h. The radiolabeled Bevacizumab preparation showed good stability in serum. After 24 h of incubation a degradation of the complex of 3 % was observed. The results are represented in Table **1**.

To assess ^{99m}Tc-HYNIC-Bevacizumab kinetic inertness under physiological conditions challenge studies were carried out by incubations this radiolabeled antibody with L-Cysteine. This incubation with L-Cysteine resulted in a significant instability of this radiocomplex. For instance, 10 and 15 % of the total radiolabeled antibody found unstable at 4 h post incubation with 0.1 and 1 mM L-Cysteine, respectively. As a control, incubations were performed simultaneously in 0.9% NaCl at 37ºC (Table **1**).

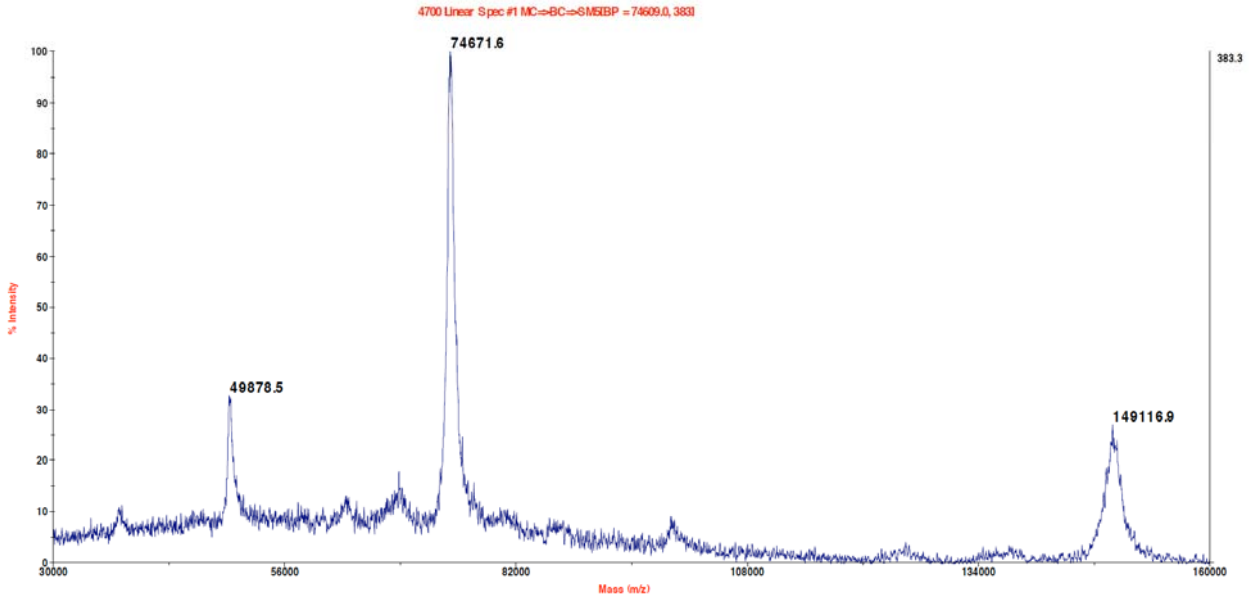

A

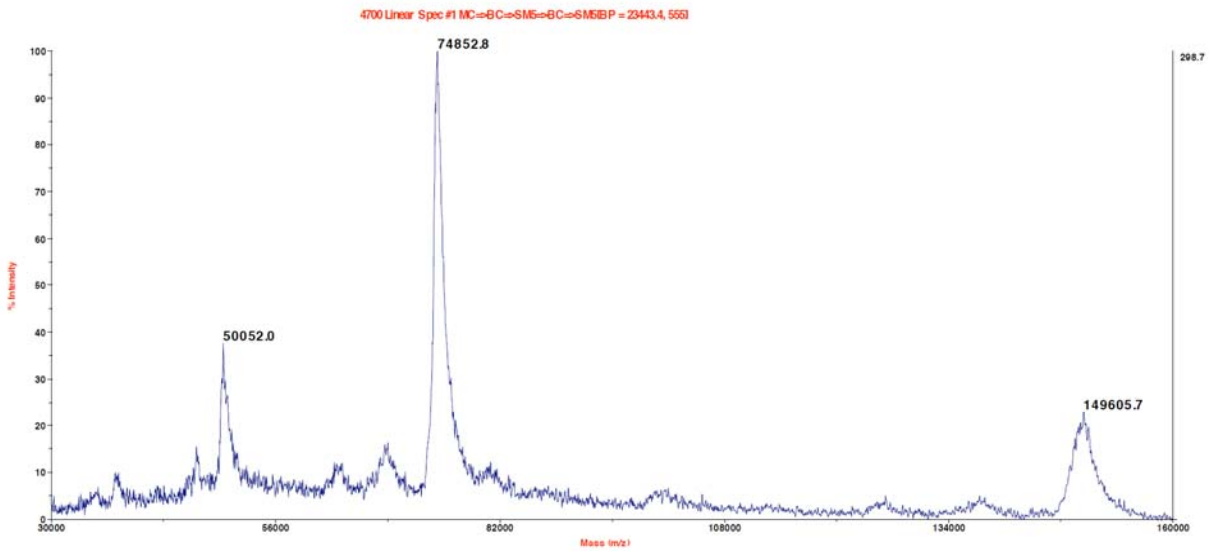

B

Figure 1: 4800 MALDI TOF/TOF (Abi Sciex) lineal acquisition was used to determine the level of HYNIC conjugation to bevacizumab. **A**) Bevacizumab, **B**) HYNIC-Bevacizumab.

These data indicate that ^{99m}Tc-HYNIC-Bevacizumab is stable in saline and serum conditions, showing signals of degradation only when co-incubated with an important amount (a great excess) of a competing ligand. L-Cysteine is a very potent ligand, known to form stable complexes with ^{99m}Tc.

3.4. *In Vivo* Biodistribution Studies and Imaging Studies

Detailed *in-vivo* pharmacokinetic studies in healthy and B16-F1 tumor-bearing C57BL/6J mice are summarized in Table **2**.

The retention of ^{99m}Tc-HYNIC-Bevacizumab was observed to be high both in liver and kidney, suggesting a mixed hepatobiliary/renal clearance for this radiotracer. The radioactivity in the kidneys of tumor-bearing mice was 7.50 ± 2.33 %ID/g, 4.87 ± 0.89 %ID/g and 4.46 ± 1.69 %ID/g at 1, 4 and 24 h, respectively. In the liver, the uptake at the same time points was 8.40 ± 1.41 %ID/g, 7.09 ± 1.06 %ID/g and 7.57 ± 0.76 %ID/g, respectively. This data was accompanied by a high percentage of the injected dose in intestine and urine. At 24 h p.i., 13.10 ± 0.43 %ID of ^{99m}Tc-HYNIC-Bevacizumab had been excreted in the urine and 3.48 ± 0.11 %ID detected in the intestines, in

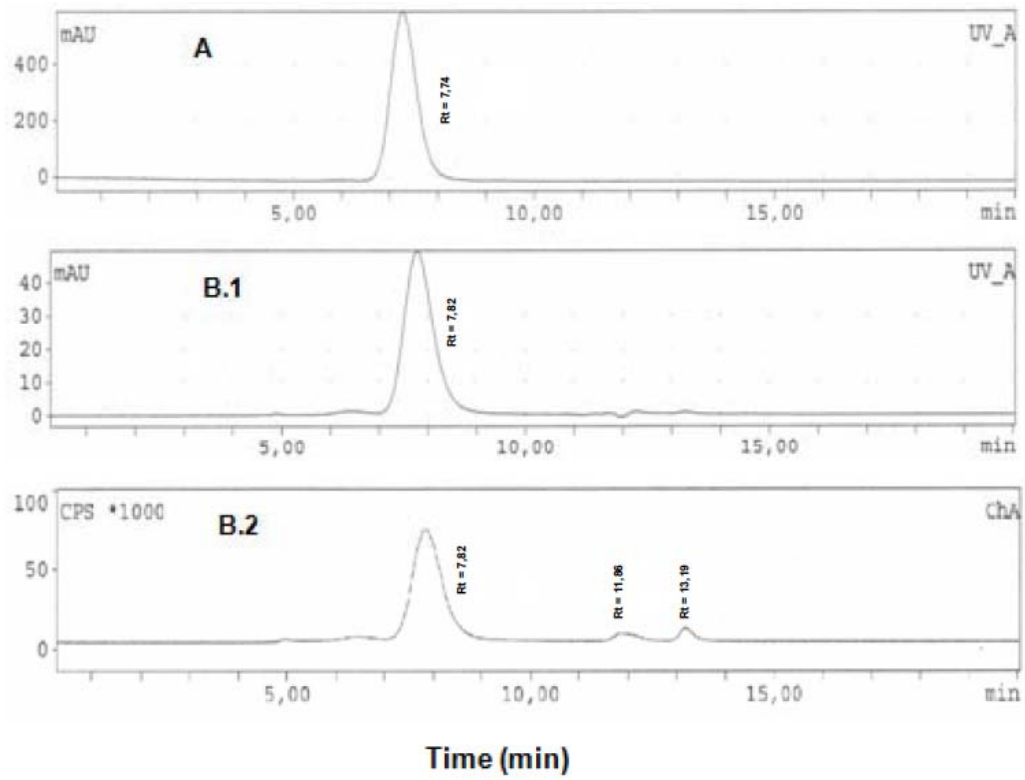

Figure 2: HPLC profile of Bevacizumab used UV detector (**A**) and [99m]Tc-HYNIC-Bevacizumab in the labeling conditions (**B.1** and **B.2**) used two detectors: UV and NaI(Tl).

Table 1: ***In-vitro*** **radiochemical stability of [99m]Tc-HYNIC-bevacizumab in 0,9% NaCl, Serum, 0.1 and 1 mM of L-Cysteine solution, at 37ºC. The HPLC measurements were obtained with a Protein-Pak 300 SW 7.5 mm x 30 cm column (Waters) with isocratic mode phosphate buffer 0.05 M, pH 7.0, 0.7 mL/min flow rate, equipped with UV absorbance and NaI(Tl) scintillation detectors**

Time (h)	%RCP NaCl 0,9% at 37ºC	%RCP 0.1mM L-Cysteine at 37ºC	%RCP 1mM L-Cysteine at 37ºC	%RCP Serum at 37ºC
0	95,50 ± 3,08	-	-	-
1	95,35 ± 2,34	93,91 ± 3,96	92,99 ± 3,32	97,97 ± 2,40
2	95,18 ± 3,44	93,14 ± 4,51	87,52 ± 5,68	95,48 ± 4,84
4	93,48 ± 5,19	84,54 ± 1,02	79,53 ± 1,56	94,35 ± 5,58
24	85,83 ± 4,56	72,63 ± 2,06	62,95 ± 3,78	92,22 ± 0,65

tumor-bearing (n=5). The value for urine includes the %ID from collected urine and also the obtained in the bladder.

Blood radioactivity levels were 27.02 ± 0.47 % ID/g at 1 h p.i., 18.21 ± 0.32 % ID/g at 4 h p.i. followed by 13.13 ± 5.80 %ID/g at 24 h p.i., which indicates a slow clearance from the blood by 24 h post injection of the antibody. In spite of the high activity in the blood, low accumulation of [99m]Tc-HYNIC-Bevacizumab is verified in various nonspecific tissues from the mice. It's worth show that there was no significant difference in the [99m]Tc-HYNIC-Bevacizumab uptake between the healthy and the tumor-bearing mice in all the organs analyzed.

The biodistribution data for tumor-bearing mice shows that the tumor had a good retention of [99m]Tc-HYNIC-Bevacizumab. One hour after its injection, tumor uptake was 4.64 ± 1.96 %ID/g followed by 5.49 ± 0.40 %ID/g four hours after its injection and 5.87 ± 0.71 %ID/g at 24 h.

These findings corroborate with the obtained by SPECT/CT studies. Representative whole-body sagital and transverse slices of C57BL/6J mice at 24 h p.i. of [99m]Tc-HYNIC-Bevacizumab are shown in Figure **3**. Despite intense activity detected in the thoracic, there is a remarkable uptake in the tumor area. This radioactivity is better visualized at 24 h, due to the higher tumor-to-blood (0.44 versus 0.17 and 0.30, at 1

Table 2: Pharmacokinetic studies of ^{99m}Tc-HYNIC-bevacizumab using healthy and tumor-bearing C57BL/6J mice at 1, 4 and 24 h p.i. Values are expressed as %ID per gram (or %ID) (mean ± SD, n=5)

	Healthy C57BL/6J mice			Tumor-bearing C57BL/6J mice		
Tissue	**1 h**	**4 h**	**24 h**	**1 h**	**4 h**	**24 h**
Percent injected dose/gram (%ID/g)*						
Blood	21,61 ± 9,36	25,44 ± 2,78	11,04 ± 2,83	27,02 ± 0,47	18,21 ± 0,32	13,13 ± 5,80
Liver	6,70 ± 1,13	8,05 ± 1,62	10,06 ± 3,79	8,40 ± 1,41	7,09 ± 1,06	7,57 ± 0,76
Hearth	2,57 ± 0,93	6,05 ± 1,18	4,94 ± 1,71	6,05 ± 0,07	3,78 ± 1,05	3,31 ± 1,46
Lungs	3,04 ± 1,55	7,89 ± 1,44	4,91 ± 2,20	4,57 ± 0,66	2,73 ± 1,87	5,78 ± 2,36
Spleen	1,34 ± 0,69	4,47 ± 0,47	3,03 ± 1,76	2,16 ± 0,41	1,59 ± 0,56	3,82 ± 1,82
Kidneys	5,32 ± 2,61	7,77 ± 1,13	4,98 ± 2,61	7,50 ± 2,33	4,87 ± 0,89	4,46 ± 1,69
Thyroid	3, 21 ± 0,51	2,91 ± 0,31	2,37 ± 0,73	1,93 ± 0,47	1,25 ± 0,89	1,66 ± 0,08
Muscle	0,77 ± 0,20	0,99 ± 0,46	0,88 ± 0,54	0,50 ± 0,28	0,32 ± 0,27	0,69 ± 0,08
Bone	0,79 ± 0,26	1,66 ± 0,34	1,44 ± 0,55	0,93 ± 1,04	0,53 ± 0,41	1,11 ± 0,09
Stomach	3,16 ± 0,77	3,01 ± 0,44	1,94 ± 0,83	2,00 ± 0,09	1,19 ± 0,72	3,50 ± 1,46
IT	1,73 ± 0,81	2,80 ± 0,23	2,95 ± 0,35	2,93 ± 1,27	1,32 ± 0,41	3,04 ± 1,03
Tumor	-	-	-	4,64 ± 1,96	5,49 ± 0,40	5,87 ± 0,71
Percent injected dose (%ID)*						
Intestine	6,38 ± 1,98	6,29 ± 0,26	5,27 ± 0,84	7,27 ± 2,48	3,06 ± 1,24	3,48 ± 0,11
Urine, bladder	4,18 ± 1,87	5,88 ± 0,73	19,59 ± 5,00	6,53± 1,06	8,80 ± 1,43	13,10 ± 0,43
Uptake ratio of tumor/normal tissue*						
Tumor/blood				0,17	0,30	0,44
Tumor/muscle				9,28	17,16	8,51

*Data are presented as %ID/g (or %ID) ± standard deviation (n=5). IT=Intestinal tract.

and 4 h) and tumor-to-muscle (8.51 versus 9.28 and 17.16, at 1 and 4 h) ratios. As expected, a substantial uptake of the radiolabelled Bevacizumab in bladder and liver was evident at all the images, as a result of the renal and hepatic function.

4. DISCUSSION

It has been demonstrated recently that radiolabeled Bevacizumab accumulates specifically in xenoengraft tumors expressing VEGF-A [31].

The aim of this study was the radiolabeling of Bevacizumab with ^{99m}Tc *via* the bifunctional coupling agent HYNIC and its radiochemical and biological evaluation as an agent for preclinical imaging studies of melanoma. It is very important in the labelling of targeting molecules with metallic radionuclides to retain the biologically activity of the molecule without affecting its physiological properties. The 6-hydrazinonicotinyl group, known as HYNIC, has been one of the bifunctional coupling agents used to bind covalently to the targeting molecule and chelate a radiometal in conjunction with a coligand. Abrams and co-workers were the first to describe the synthesis and *in vivo* evaluations of the bioconjugates [42].

In this work we have looked for an alternative methodology to obtain Suc-HYNIC. The synthesis of Suc-HYNIC was performed using the method described previously with some modifications [42]

Most of radiopharmaceuticals currently available in clinical nuclear medicine are ^{99m}Tc compounds due to the favourable physical imaging characteristics of ^{99m}Tc (6 h half-life, monochromatic 140 KeV photons). Furthermore, ^{99m}Tc is readily available from the ^{99}Mo-^{99m}Tc generators at low cost. ^{99m}Tc radiopharmaceuticals have been a cornerstone of nuclear medicine over the last decades. It´s use is preferred over ^{111}In on account of better imaging properties, lower radiation dose and cost. In this sense, we evaluated the efficacy of ^{99m}Tc-labeled Bevacizumab for imaging studies of melanoma. Other groups also showed that the labelling of monoclonal antibodies against VEGF allows its detection in tumors [31,33,35,41,43].

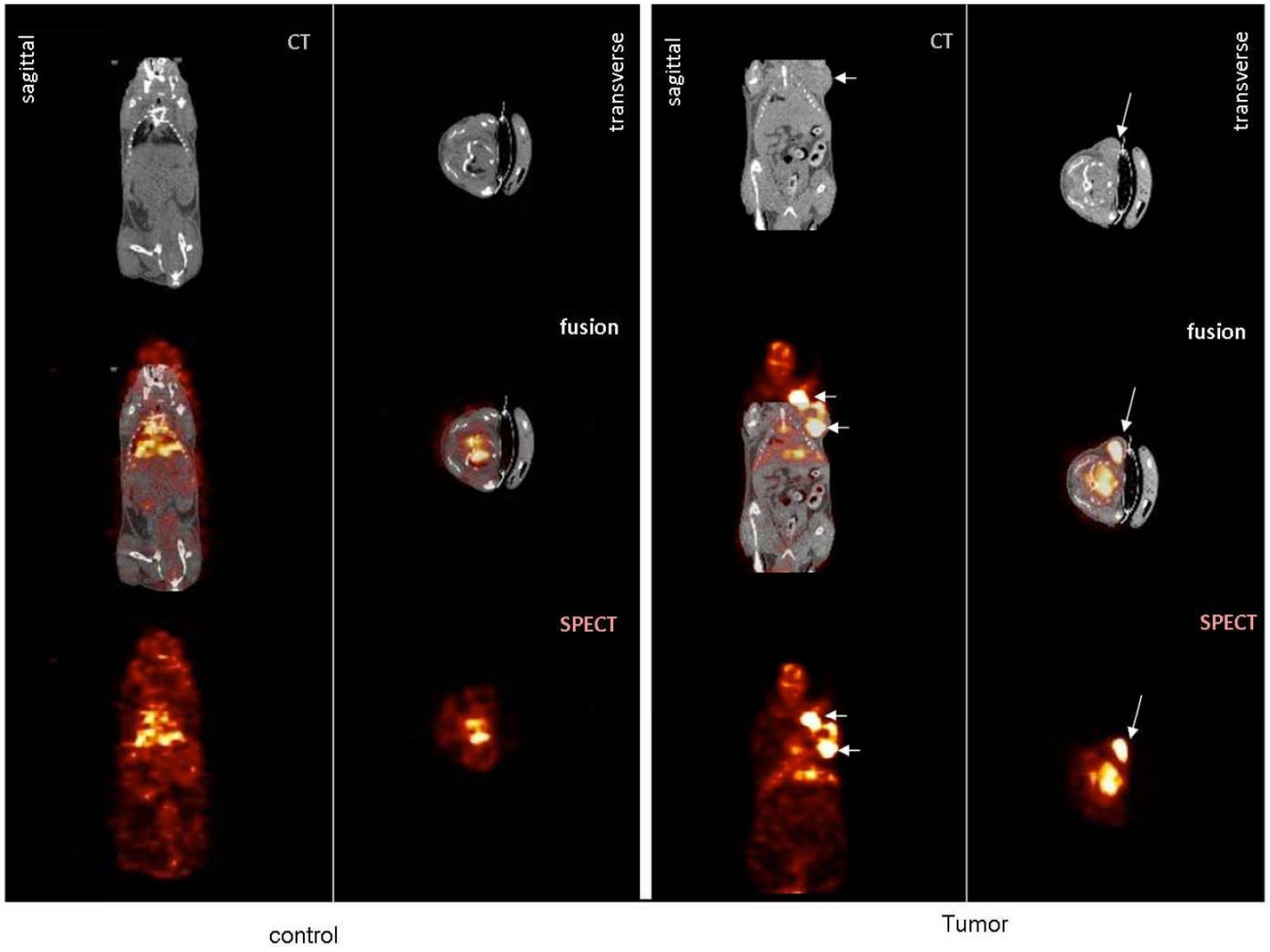

Figure 3: SPECT/CT images on healthy and tumor-bearing C57BL/6J mice at 24 h post-injection of ^{99m}Tc-HYNIC-Bevacizumab, the animals (n=3 per time) were anesthetized with a gas mixture (air and 1–1.5% isoflurane) and submitted to SPECT/CT images. Images data were acquired using HRES collimators with 1.4mm, 127x127 mm trans-axial field of view, 64 projections with >9Kctps each all animals with an Triumph microSPECT/CT (Gama Medica). All acquired images were analyzed by Amide with same threshold parameters (75%) for data interpretation [40]. There is a remarkable uptake of the radiolabeled bevacizumab in the right arm (white arrows), site of the tumor, which is observed only in tumor-bearing mice.

In the present study, labelling of Bevacizumab with ^{99m}Tc was done after a simple 30 minutes conjugation with the Suc-HYNIC group. Bevacizumab could be labelled with ^{99m}Tc in a rapid and simple method with high radiolabeling efficiency and fast quality controls. After labeling with ^{99m}Tc, a stable radiolabel antibody was obtained as shown by a low level of degradation products, in particular pertechnetate, after 24 h *in vitro* incubation in saline, as well as in serum. Also we found that the exposition of the labeled complex to a L-Cysteine concentration of 0.1 and 1 mM during 4 h showed less than ≤ 3 and % of free $^{99m}TcO_4^-$, respectively.

The *in vivo* stability was also verified through biodistribution studies with healthy and tumor mice at 1, 4 and 24 h. There was a slow clearance, with elimination primarily *via* the liver and to a lesser extent the kidneys, with lower uptake in other not target organs. The significant accumulation of radioactivity found in liver, indicates that the primary route of clearance was hepatobiliary. However at 24 hours a moderate percent of the injected dose is eliminated in urine and bladder and a significant amount was detected in the intestines. Nonspecific binding of radiolabeled proteins in kidneys often occurs *in vivo* [44]. High levels of radioactivity in the kidneys could be attributed to the degraded forms of the radiolabel antibody, a result of lysosomal degradation of the antibody with long residence times within renal cells and slow clearance from the lysosome [45-47]. Methods to minimize this non-specific renal retention of radiolabel antibodies are under investigation.

The radioactivity detected in the lung might be a contribution of its intense blood pool activity, since this is a highly blood-perfused organ [48].

The high activity detected in the blood over the times observed, could be due to the relatively long biological half-life of antibodies in the bloodstream. Bevacizumab has a mean half-life of approximately three weeks (17-21 days), which results in a notable blood pool activity in organs highly vascularised, including hearth and lungs, as well as a compromised tumor-to-blood ratio in nuclear medicine imaging studies.

VEGF, the target molecule of the humanized antibody Bevacizumab, is not only a key regulator of tumour angiogenesis, but also plays an important role in the physiology of the normal vasculature. Its expression is noted in the parenchyma of various organs in healthy animals including kidneys, liver, lung and spleen [49] and, therefore, it`s expected that VEGF-targeted agents bind to such non-tumour tissues.

The non-tumor uptake, combined with the low blood clearance, confers a limitation in regards to the imaging of tumors localized in regions endowed with a basal affinity to the antibody. Nevertheless, even with a relatively low tumor-to-blood ratio, Bevacizumab uptake is clear in tumors that do not overlay with such functional organs, as can be seen by the SPECT/CT images.

SPECT/CT studies performed in animals bearing subcutaneous murine melanoma in left lateral of thorax showed a favourable uptake of Bevacizumab in the tumor, suggesting that this human monoclonal antibody has not only affinity for human tissues, but also for murine specimens. This affinity was previously confirmed by immunoassays performed on B16-F10 tumor samples. Western blot analyses revealed that Bevacizumab recognizes the same labeling pattern of bands that the obtained by conventional polyclonal and monoclonal antibodies [42]. Also, fluorescent analysis of murine C57BL/6J melanoma cryosections with FITC-Bevacizumab showed a clear pattern of stain in the tissue [42].

These results led us to believe that this antibody could be used as an approach for tumor nuclear imaging in clinical studies. This should be useful to provide insights of the angiogenic stimulus before and after chemotherapy, which might help improve current antitumor therapy. Therefore, the humanized Bevacizumab configures an encouraging potential tool for imaging strategies for the non-invasive monitoring of VEGF-status in solid tumors.

CONCLUSIONS

We developed a simple synthesis method to obtain Suc-HYNIC used as an bifunctional coupling agent for ^{99m}Tc-labeling. The ^{99m}Tc-HYNIC-Bevacizumab was obtained with radiochemical purity greater than 90% that remains stable throughout the observation time. The same could be quickly and easily controlled by different chromatographic systems. SPECT/CT images enabled good visualization of the tumour as early as 6 h p.i., significantly improved within 24 h. Therefore, ^{99m}Tc-HYNIC-Bevacizumab could become a potential radiopharmaceutical to evaluate the expression of vascular endothelial growth factor (VEGF) in solid tumors and then decide if this can be treated or not with this high-cost drug. ^{99m}Tc-HYNIC-Bevacizumab could be seen as a clinic tool for the screening of solid tumors that might respond to the bevacizumab chemotherapy.

ACKNOWLEDGEMENTS

The authors are grateful to Roche® for providing Avastin® and CSIC. This work was supported in part by Camacho, X and García, M.F. fellowships from Agencia Nacional de Investigación e Innovación (ANII, Uruguay). No potential conflict of interest relevant to this article was reported.

SUPPLEMENTAL DATA

The supplemental data can be downloaded from the journal website along with the article.

REFERENCES

[1] Folkman J. Tumor Angiogenesis; therapeutics implications. N Engl J Med 1971; 285: 1182-86. http://dx.doi.org/10.1056/NEJM197111182852108

[2] Folkman J. Angiogenic factors. Science 1987; 235: 442-47. http://dx.doi.org/10.1126/science.2432664

[3] Folkman J. What is the evidence that tumors are angiogenesis dependent? J Natl Cancer Inst 1990; 82: 4-6. http://dx.doi.org/10.1093/jnci/82.1.4

[4] Dvorak HF. Angiogenesis. J Thromb Haemost 2005; 3: 1835-42. http://dx.doi.org/10.1111/j.1538-7836.2005.01361.x

[5] Carmeliet P. Angiogenesis in life, disease and medicine. Nature 2005; 438: 932-36. http://dx.doi.org/10.1038/nature04478

[6] Shibuya M. Stucture and fuction of VEGF/VEGF-receptor system involved in angiogenesis. Cell Sturct Funct 2001; 26: 25-35. http://dx.doi.org/10.1247/csf.26.25

[7] Ferrara N. Molecular and biological properties of vascular endothelial growth factor. J Mol Med 1999; 77: 527-43. http://dx.doi.org/10.1007/s001099900019

[8] Ferrara N. Role of vascular endothelial growth factor in regulation of physiological angiogenesis. Am J Physiol Cell Physiol 2001; 280: 1358-66.

[9] Ferrara N. Role of vascular endothelial growth factor in physiologic angiogenesis: therapeutic implications. Semin Oncol 2002; 29: 10-14.

[10] Ferrara N. Vascular endothelial growth factor: basic science and clinical progress. Endocr Rev 2004; 25: 581-11. http://dx.doi.org/10.1210/er.2003-0027

[11] Ferrara N, Davis-Smyth T. The biology of Vascular endothlial growth factor. Endocrine Rev 2008; 18: 4-25. http://dx.doi.org/10.1210/edrv.18.1.0287

[12] Folkman J. Angiogenesis in cancer, vascular, rheumatoid and other desease. Nat Med 1995; 1: 27-31. http://dx.doi.org/10.1038/nm0195-27

[13] Ferrara N, Gerber HP, Le Couter J. The biology of VEGF and its receptors. Natl Med 2003; 9(6): 669-76. http://dx.doi.org/10.1038/nm0603-669

[14] Hoeben A, Landuyt B, Highley M, Wildier H, Van Oosterom A, De Bruijn E. Vascular endothelial growth factor and angiogenesis. Pharmacol Rev 2004; 56: 549-80. http://dx.doi.org/10.1124/pr.56.4.3

[15] Veikkola T, Karkkainen M, Cleasson-Welsh L, Alitalo K. Regulation of angiogenesis via vascular endothelial growth factor receptors. Cancer Res 2000; 60: 203-12.

[16] Shibuya M. Vascular endothelial growth factor receptor-2: its unique signaling and specific ligand, VEGF-E. Cancer Sci 2003; 94: 751-6. http://dx.doi.org/10.1111/j.1349-7006.2003.tb01514.x

[17] Crawford SE. Vascular interference: a blockade to tumor epithelial growth. Hepatology 2004; 39: 1491-4. http://dx.doi.org/10.1002/hep.20278

[18] Park JE, Keller GA, Ferrara N. The vascular endothelial growth factor (VEGF) isoforms: differential deposition into the subepithelial extracellular matrix and bioactivity of extracellular matrix-bound VEGF. Mol Biol Cell 1993; 4: 1317-26. http://dx.doi.org/10.1091/mbc.4.12.1317

[19] Dvorak HF. Vascular permeability factor/vascular endothelial growth factor: a critical cytokine in tumor angiogenesis and a potential target for diagnosis and therapy. Am Soc Clin Oncol 2002; 20: 4368-80. http://dx.doi.org/10.1200/JCO.2002.10.088

[20] Rosen LS. VEGF-targeted therapy: terapeutics potential and recent advances. Oncologist 2005; 10: 382-91. http://dx.doi.org/10.1634/theoncologist.10-6-382

[21] Gerber HP, Ferrara N. Pharmacology and pharmacody-namics of bevacizumab as monotherapy or in combination with cytotoxic therapy in preclinical studies. Cancer Res 2005; 65: 671-80.

[22] Presta LG, Chen H, O'Connor SJ, Chisholm V, Meng YG, Krummen L, *et al*. Humanization of an anti- vascular endothelial growth factor monoclonal antibody for the therapy of solid tumors and other disorders. Cancer Res 1997; 57: 4593-99.

[23] Hurwitz H, Fehrenbacher L, Novotny W, Cartwright T, Hainsworth J, Heim W, *et al*. Bevacizumab plus irinotecan, fluorouracil, and leucovorin for metastic colorectal cancer. N Engl J Med 2004; 350: 2335-42. http://dx.doi.org/10.1056/NEJMoa032691

[24] Stahl J, Bar-Meir E, Friedman E, Regev E, Orenstein A, Winkler E. Genetics in melanoma. Isr Med Assoc J 2004; 6: 774-7.

[25] Gorski DH, Leal AD, Goydos JS. Differential expression of vascular endothelial growth factor-A isoforms at different stages of melanoma progression. J Am Coll Surg 2003; 197: 408-18. http://dx.doi.org/10.1016/S1072-7515(03)00388-0

[26] Tas F, Duranyildiz D, Oguz H, Camlica H, Yasasever, Topuz E. Circulating serum levels of angiogenic factors and vascular endothelial growth factor receptors 1 and 2 in melanoma patients. Melanoma Res 2006; 16: 405-11. http://dx.doi.org/10.1097/01.cmr.0000222598.27438.82

[27] Ferlay J, Parkin F, Pisani P, Parkin DM. Globocan 2002: Cancer Incidence, Mortality and Prevalence Worldwide. Lyon: IARC 2004; 147.

[28] Sekulic A, Haluska P Jr, Miller AJ, Genebriera De Lamo J, Ejadi S, Paulido JS, *et al*. Malignant melanoma in the 21st century: the emerging molecular landscape. Mayo Clin Proc 2008; 83: 825-46. http://dx.doi.org/10.4065/83.7.825

[29] Fidler IJ. The biology of melanoma metastasis. J Dermatol Surg Oncol 1998; 14: 875-81. http://dx.doi.org/10.1111/j.1524-4725.1988.tb03591.x

[30] Jain RK, Duda DG, Clark JW, Loeffler JS. Lessons from phase III clinical trials on anti-VEGF therapy for cancer. Nat Clin Oncol 2006; 3: 24-40. http://dx.doi.org/10.1038/ncponc0403

[31] Nagengast WB, Vries EG, Hospers GA, Mulder NH, Jong JR, Hollem H, *et al*. *In vivo* VEGF imaging with radiolabeled Bevacizumab in a human ovarian tumor xenograft. J Nucl Med 2007; 48: 1313-19. http://dx.doi.org/10.2967/jnumed.107.041301

[32] Stollman TH, Scheer MG, Leenders WP, Verrijp KC, Soede AC, Oyen WJ, *et al*. Specific imaging of VEGF-A expression with radiolabelled anti-VEGF monoclonal antibody. Int J Cancer 2008; 122: 2310-4. http://dx.doi.org/10.1002/ijc.23404

[33] Stollman TH, Scheer MG, Franssen GM, Verrijp KC, Soede AC, Oyen WJ, *et al*. Tumor accumulation of radiolabelled bevacizumab due to targeting of cell- and matrix-associated VEGF-A isoforms. Cancer Biother Radiopharm 2009; 24: 195-200. http://dx.doi.org/10.1089/cbr.2008.0574

[34] Chang SK, Rizvi I, Solban N, Hasan T. *In vivo* optical molecular imaging of vascular endothelial growth factor for monitoring cancer treatment. Clin Cancer Res 2008; 14: 4146-53. http://dx.doi.org/10.1158/1078-0432.CCR-07-4536

[35] Scheer MG, Stollman TH, Boerman OC, Verrijp K, Sweep FC, Leenders WP, *et al*. Imaging liver metastases of colorectal cancer patients with radiolabelled bevacizumab: lack of correlation with VEGF-A expression. Eur J Cancer 2008; 44: 1835-40. http://dx.doi.org/10.1016/j.ejca.2008.05.026

[36] Jurisson S, Berning D, Jia W, Ma D. Coordination Compounds in Nuclear Medicine. Chem Rev 1993; 93: 1137-56. http://dx.doi.org/10.1021/cr00019a013

[37] Rennen HJ, Boerman OC, Koenders EB, Oyen WJ, Corstens FH. Labeling proteins with Tc-99m via Hydrazinonicotinamide (HYNIC): Optimization of the conjugation reaction. Nucl Med Biol 2000; 27: 599-604. http://dx.doi.org/10.1016/S0969-8051(00)00134-7

[38] Meszaros LK, Dose A, Biagini SCG, Blower PJ. Hydrazinonicotinic acid (HYNIC)-Coordination chemistry and applications in radiopharmaceutical chemistry. Inorg Chim Acta 2010; 363: 1059-69. http://dx.doi.org/10.1016/j.ica.2010.01.009

[39] Hantowich DJ, Virzi F, Forgarasi M, Rusckowski M, Winnard P. Can a Cysteine Challenge Assay Predict the *In vivo* Behavior of 99mTc-labeled Antibodies? Nuc Med Biol 1994; 21: 1035-44. http://dx.doi.org/10.1016/0969-8051(94)90175-9

[40] Loening AM, Gambhir SS. AMIDE: A Free Software Tool for Multimodality Medical Image Analysis. Mol Imag 2003; 2(3): 131-37. http://dx.doi.org/10.1162/153535003322556877

[41] Camacho X, García MF, Calzada V, Fernández M, Moreno M, De Aguiar R, *et al*. [99mTc(CO)3]-radiolableled Bevacizumab: *in vitro* and *in vivo* evaluation in melanoma model. Oncology 2013; 82: 200-209. http://dx.doi.org/10.1159/000338961

[42] Abrams MJ, Juweid M, tenKate CI, Schwartz DA, Hauser MM, Gaul FE, *et al*. Technetium-99m-Human Polyclonal IgG Radiolabeled via the Hydrazino Nicotinamide Derivatives for Imaging Focal Sites of Infection in Rats. J Nuc Med 1990; 31: 2022-18.

[43] Camacho X, García MF, Calzada V, Fernández M, Porcal W, Alonso O, *et al*. Synthesis and evaluation of 99mTc chelate-conjugated Bevacizumab. Curr Radiopharm 2013; 6: 12-19. http://dx.doi.org/10.2174/1874471011306010003

[44] Gotthardt M, van Eerd-Vismale J, Oyen WJ, de Jong M, Zhang H, Rolleman E, *et al*. Indication for different mechanisms of kidney uptake of radiolabeled peptides. J Nucl Med 2007; 48: 596-601. http://dx.doi.org/10.2967/jnumed.106.036020

[45] Akizawa H, Uehara T, Arano Y. Renal uptake and metabolism of radiopharmaceuticals derived from peptides and proteins. Adv Drug Deliv Rev 2008; 60: 1319-28. http://dx.doi.org/10.1016/j.addr.2008.04.005

[46] Tsai SW, Li L, Williams LE, Anderson AL, Raubitscheck AA, Shively JE. Metabolism and renal clearance of 111In-labeled DOTA-conjugated antibody fragments. Bioconjug Chem 2001; 12: 264-70. http://dx.doi.org/10.1021/bc0000987

[47] Rogers BE, Franano FN, Duncan JR, Edwarda WB, Anderson CJ, Connett JM, Welch MJ. Identification of metabolites of 111In-diethylenetriaminepentaacetic acid-monoclonal antibodies and antibody fragments *in vivo*. Cancer Res 1995; 55: 5714s-20s.

[48] Kumar SR, Quinn TP, Deutscher SL. Evaluation of an 111In-radiolabeled peptide as a targeting and imaging agent for Erb-2 receptor expressing breast carcinomas. Clin Cancer Res 2007; 13: 6070-9. http://dx.doi.org/10.1158/1078-0432.CCR-07-0160

[49] Monacci WT, Merrill MJ, Oldfield EH. Expression of vascular permeability factor/vascular endothelial growth factor in normal rat tissues. Am J Physiol 1993; 264(4 Pt 1): C995-1002.

Received on 10-01-2014 Accepted on 03-02-2014 Published on 18-02-2014

http://dx.doi.org/10.6000/1927-7229.2014.03.01.9